# α-MnO₂ hollow clews for rechargeable Li-air batteries with improved cyclability

ZHANG LeiLei[1,2], WANG ZhongLi[1], XU Dan[1], XU JiJing[1], ZHANG XinBo[1*] & WANG LiMin[1*]

[1] *State Key Laboratory of Rare Earth Resource Utilization, Changchun Institute of Applied Chemistry, Chinese Academy of Sciences, Changchun 130022, China;*
[2] *Graduate University of Chinese Academy of Sciences, Beijing 100049, China*

Lithium-air (Li-air) batteries have attracted worldwide attention due to their high energy density (11140 Wh kg$^{-1}$) comparable to gasoline. In this work, we have synthesized the α-MnO₂ hollow clews via a simple method and characterized them by X-ray diffraction and scanning electron microscope. Interestingly, cycle performance of Li-air batteries is improved greatly when using the α-MnO₂ hollow clews as the catalyst. The first discharge capacity is 596 mAh g$^{-1}$, and the charge capacity is 590 mAh g$^{-1}$ at the current density of 0.1 mA cm$^{-2}$ between 2.0 and 4.2 V using the Vulcan XC-72 as the carbon material. Additionally, by reassembling new batteries with the used lithium foil, separators and cathode separately, we find that the cathode is the key role to end the Li-air battery life.

**Li-air battery, α-MnO₂, catalyst, cyclability**

The rapid depletion of finite fossil-fuel and global warming linked to carbon dioxide emissions make the development of clean energy storages a worldwide imperative. Among all advanced battery systems, Li-air batteries have the highest theoretical specific energy of 11140 Wh kg$^{-1}$ comparable to one of the most energy-dense common liquids-gasoline [1–3]. In practical, Li-air batteries have the potential to provide gravimetric energy three times, or greater, than that of conventional Li-ion batteries [4–8]. Therefore, Li-air batteries have attracted worldwide attention [9–16] since the non-aqueous electrolyte Li-air battery is first reported by Abraham and Jiang [4], especially after the attractive rechargeability is demonstrated in 2006 [1].

A typical design for non-aqueous Li-air battery contains a Li metal anode, a conducting porous carbon supported cathode, a separator and an aprotic electrolyte. The funda-

mental discharge reaction is thought to be: $2Li + O_2 = Li_2O_2$ ($E = 2.96$ V). However, for most of current Li-air batteries, the discharge potential is approximately 2.6 V and the charge potential is above 4.0 V [17–19]. This overpotential between the discharge and charge severely reduces the cycle electrical energy efficiency. Another, the discharge products $Li_2O_2$ are not soluble in the organic electrolyte and deposit in the carbon-based porous cathode, which increases the polarization and blocks further intake of oxygen, thus leading to the end of the battery life. There are also many other obstacles that must be overcome to improve the cycle performance, including the instability and volatility of organic electrolyte, the corrosion of lithium metal anode, the air breathable separators, and the efficiency of catalysts.

It is generally believed that catalysts could raise the discharge potential, drop the charge potential and thus increase the round trip efficiency and ultimately improve the cyclic performance. Therefore, effective catalysts are urgently

*Corresponding authors (email: xbzhang@ciac.jl.cn; lmwang@ciac.jl.cn)

needed to improve the performance of rechargeable Li-air batteries. Recently, manganese oxides are the most widely used catalysts for rechargeable Li-air batteries, such as $\alpha$-MnO$_2$ nanowires [20], $\alpha$-MnO$_2$ nanorods [21], $\gamma$-MnO$_2$ [22,23], $\gamma$-MnOOH [24], MnO$_x$/C [25], MnO$_2$ nanoflakes [26], etc. However, the $\alpha$-MnO$_2$ hollow clews assembled with nanowires for Li-air batteries have not been reported. In this study, we synthesize the $\alpha$-MnO$_2$ hollow clews as the catalyst for Li-air batteries by a simple redox reaction and study their catalytic effect for improving the battery performance.

# 1   Experimental

## 1.1   Catalyst material synthesis and characterization

$\alpha$-MnO$_2$ hollow clews were synthesized using a redox reaction of manganese sulphate and potassium permanganate. In brief, 0.6 g KMnO$_4$ (Beijing Chemical Works, AR) and 1.1 g MnSO$_4$·H$_2$O (Aladdin Reagent, AR) were dissolved in 20 mL hot distilled water (80°C) separately. Then the manganese sulphate solution was added to the potassium permanganate solution slowly under magnetic stirring at 80°C and kept stirring for 4 h. When the solution cooled to room temperature, the black brown products were collected by centrifugation at 8000 r/min, washed three times with distilled water and followed by drying overnight at 80°C.

The structure of the prepared material was analyzed with powder X-ray diffraction (XRD) using Rigaku-Dmax 2500 diffractometer with a CuK$\alpha$ X-ray radiation. Scanning electron microscope (SEM) was performed by a Hitachi S-4800 filed emission scanning electron microscope to study the morphology of the material.

## 1.2   Electrochemical measurements

The cathodes were prepared by soaking the nickel foams (12 mm in diameter) into the slurry mixture of Vulcan XC-72 carbon (Cabot Corp.), as prepared $\alpha$-MnO$_2$ catalyst (with or without) or commercial electrolytic MnO$_2$ (EMD, Aladdin Reagent, AR), and polyvinylidene fluoride (DuPont Company, 99.9%) binder with a weight ratio of 85∶5∶10 or 85∶15. The disks of cathodes were dried at 120°C under vacuum for 12 h to evaporate the *N*-methyl-2-pyrrolidinone (Aladdin Reagent, AR) solvent. The Li-air battery consisted of a lithium metal foil anode (13 mm in diameter, 0.5 mm in thickness), two pieces of Celgard 2400 separators and as-prepared cathode, with 1 mol/L LiClO$_4$ 1∶2 by volume propylene carbonate/dimethoxyethane as electrolyte. All batteries were assembled and disassembled in an Ar-filled glove box with H$_2$O and O$_2$ content below 1 ppm. The battery performance was tested between 2.0 and 4.2 V at a constant current of 0.1 mA cm$^{-2}$ in room temperature, using LAND CT2001A multi-channel battery testing system. Be-

fore each test, the batteries rested for 4 h to reach equilibrium of oxygen concentrations and moisture of electrolyte. To avoid the negative effect from environmental contaminants, the batteries were tested in dry pure oxygen atmosphere.

Electrochemical impedance spectra of the batteries were measured by ac impedance on a BioLogic VMP3 station over the frequency range of 0.1–10$^5$ Hz with amplitude of 5 mV. SEM was used to check the cathode morphology after discharge test.

# 2   Results and discussion

## 2.1   Characterization of $\alpha$-MnO$_2$

Figure 1 shows the XRD pattern of the as-synthesized $\alpha$-MnO$_2$ powder. The characteristic peaks at 13°, 18°, 29°, 38°, 42°, 50°, 57° and 61° can be assigned to $\alpha$-MnO$_2$ phase [27]. The morphology of the $\alpha$-MnO$_2$ powder is shown in Figure 2. Figure 2(a) shows that the $\alpha$-MnO$_2$ powder consists of many round hollow clews with diameter of 3–5 $\mu$m. The magnifying images of the hollow clew shown in Figure 2(b) and (c) indicate that the hollow clews are assembled with many small nanowires.

## 2.2   Performance of Li-air battery

To investigate the catalytic effect of the $\alpha$-MnO$_2$ with the specific morphology for Li-air batteries, we add 5 wt% of the $\alpha$-MnO$_2$ powder as catalyst for Li-air batteries and tested the discharge-charge performance cycled at 2.0–4.2 V versus Li/Li$^+$. An initial discharge capacity of 596 mAh g$^{-1}$ with high reversible charge capacity of 590 mAh g$^{-1}$ is exhibited in Figure 3(a). The charge plateau is below 4.0 V in the first cycle. But the charge plateau increases, and the charge capacity decreases with the increasing cycle time. This phenomenon is reported to be due to the cathode polarization [18]. The battery might be in the process of activation
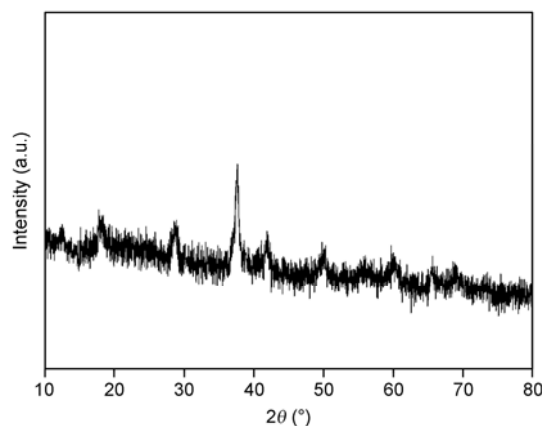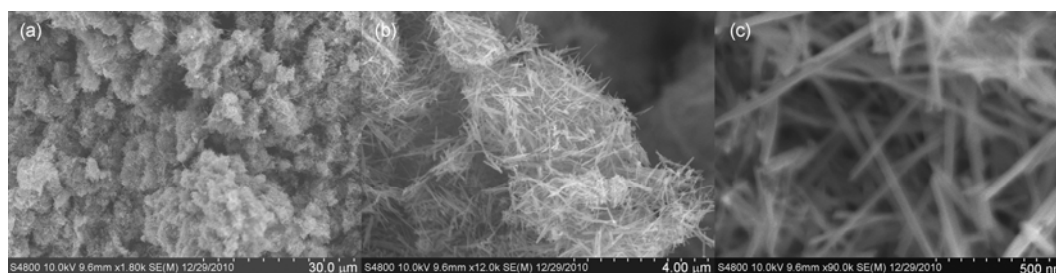


**Figure 1**   XRD pattern of the as-synthesized $\alpha$-MnO$_2$.

**Figure 2**    SEM images of the as-synthesized $\alpha$-MnO$_2$. Scale bar: (a) 30 μm; (b) 4 μm; (c) 500 nm.
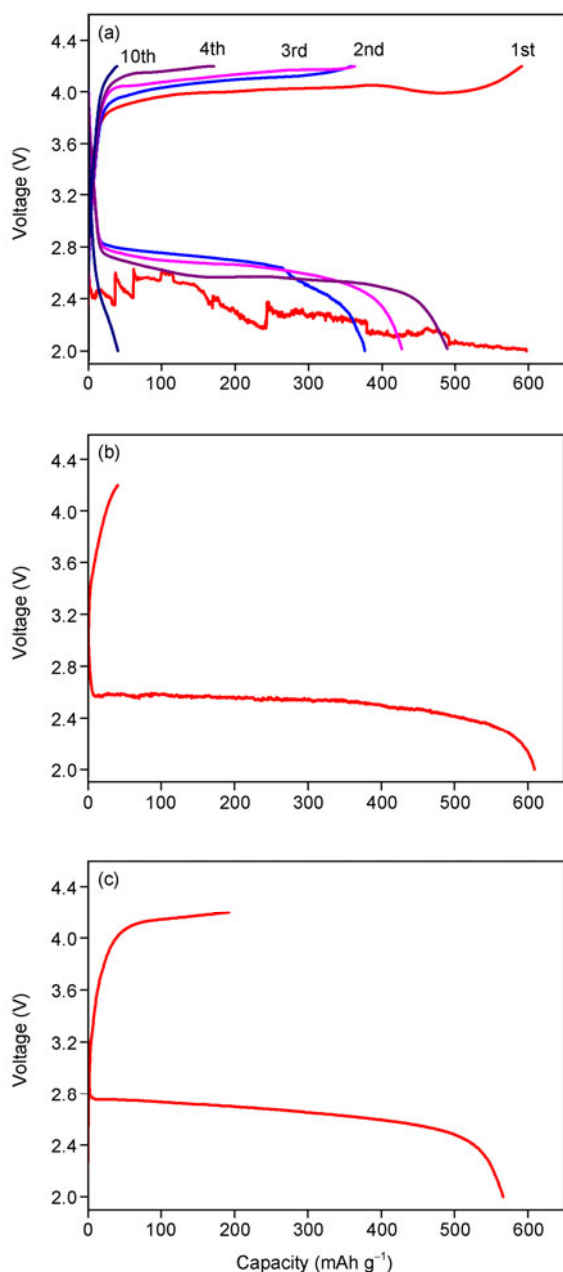


**Figure 3**    The cycle performance of the Li-air battery with the $\alpha$-MnO$_2$ hollow clews as catalysts (a), the typical discharge-charge profile of the Li-air battery with (b) pure Vulcan XC-72, and (c) EMD in the 2.0–4.2 V voltage window at 0.1 mA cm$^{-2}$.

during the first discharge, which results in fluctuation of the first discharge curve. Figure 3(b) is the typical discharge-charge curve of the Li-air battery with only Vulcan XC-72. Like the battery with $\alpha$-MnO$_2$, the open-circuit voltage (OCV) of the battery is about 2.97±0.18 V, and the discharge plateau is about 2.7 V. It is clearly that the OCV, first discharge capacity and discharge plateau of the battery with $\alpha$-MnO$_2$ catalyst do not increase obviously. However, the cycle performance improves greatly when adding 5 wt% $\alpha$-MnO$_2$ hollow clews as catalysts. The charge capacity increases from several decades to 590 mAh g$^{-1}$ and still reaches 364 mAh g$^{-1}$ after three cycles. The discharge capacity remains above 300 mAh g$^{-1}$ after 3 cycles, while the battery without $\alpha$-MnO$_2$ even does not discharge again. To further investigate the catalytic activity of MnO$_2$, we compared the Li-air battery performance between $\alpha$-MnO$_2$ hollow clews and EMD. And the results are shown in Figure 3(c). It is obviously that the discharge capacity and plateau are similar with that of $\alpha$-MnO$_2$ hollow clews. However, the charge capacity is just 193 mAh g$^{-1}$ which is much lower than the discharge capacity of 566 mAh g$^{-1}$, and the charge plateau is above 4.0 V. The reversibility of EMD is better than that of pure carbon which proves the catalytic effect of EMD. But the catalytic activity of the synthesized $\alpha$-MnO$_2$ hollow clews is much higher than that of EMD.

Figure 4 shows the initial discharge curves of Li-air batteries with $\alpha$-MnO$_2$ as catalysts at various discharge rates of 0.05, 0.1, 0.2, and 0.3 mA cm$^{-2}$. The cell discharges a capacity of 802 mAh g$^{-1}$ at a relatively low current density of 0.05 mA cm$^{-2}$. However, the specific capacity and discharge plateau drop significantly with the increasing discharge current density. The capacity decreases to 544 mAh g$^{-1}$ at 0.1 mA cm$^{-2}$, 469 mAh g$^{-1}$ at 0.2 mA cm$^{-2}$, and only 224 mAh g$^{-1}$ at 0.3 mA cm$^{-2}$. This phenomenon links with the oxygen solubility and diffusivity, which limit the discharge reaction at high current rate.

## 2.3    Investigation of Li-air battery after charge-discharge cycling

The specific capacity of the Li-air battery decreases to below 100 mAh g$^{-1}$ after 10 cycles even with the $\alpha$-MnO$_2$
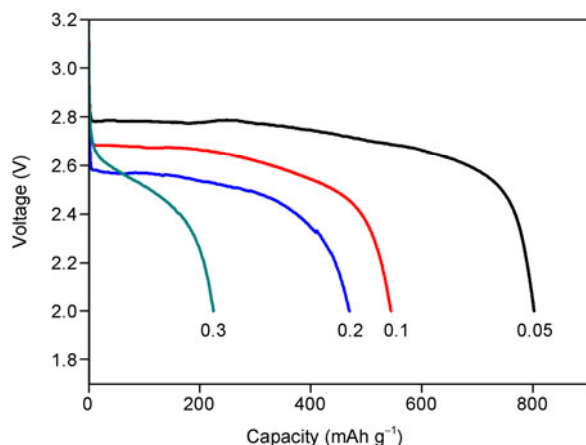
**Figure 4** The initial discharge curves of Li-air batteries with α-MnO₂ as catalysts in the 2.0–4.2 V voltage window at various discharge rates: 0.05, 0.1, 0.2, and 0.3 mA cm⁻².
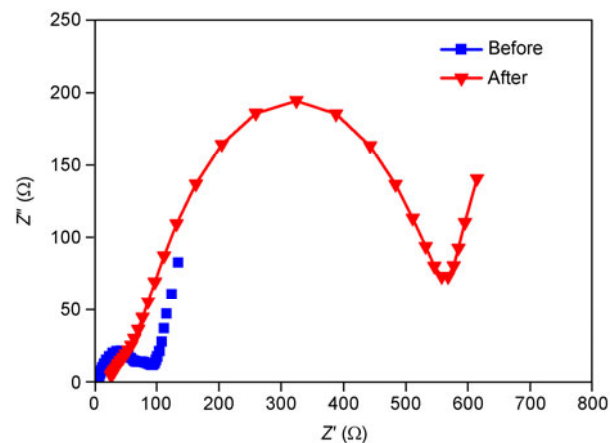


**Figure 5** Impedance spectra of the Li-air battery before and after 10 cycles.

catalyst. As the lithium metal foil, separator and carbon cathode are three main components of a Li-air battery, to investigate which one is the most important factor might be responsible for the degrade of the battery, we re-assembled new batteries with the used lithium metal foil, separators, and cathode of the battery after 10 cycles and tested their discharge capacity. As illustrated in Table 1, the discharge capacities are 819 and 541 mAh g⁻¹ for batteries with the used lithium metal foil and separators, respectively. However, the discharge capacity of the battery with the used cathode is only 27 mAh g⁻¹, indicating that the cathode is the key factor to end the battery life. Although the surface of a discharged lithium metal foil partly changes to black and the Celgard 2400 separators cannot prevent O₂ well, they are found to have little effect on the battery performance in our experiment.

Figure 5 shows the impedance behaviors of the Li-air battery before and after 10 cycles. The semicircle at high frequencies relates to the contact resistance and the discharged product layer, and the inclined line in low frequencies can be related the ion diffusion within the cell. Clearly, the resistance of the cell increases greatly after cycles. During discharge, the poor electronic conductive products deposit on the initial cathode material, which can be seen clearly from the SEM images before and after discharge (Figure 6). These slack deposits on the surface of carbon materials reduce the electronic conductivity of the cathode, which leads to the increase in resistance and polarization. This may be the most important factor that leads to the degradation of the cathode.

**Table 1** The discharge capacity of the batteries assembled with separate components of the cycled cell

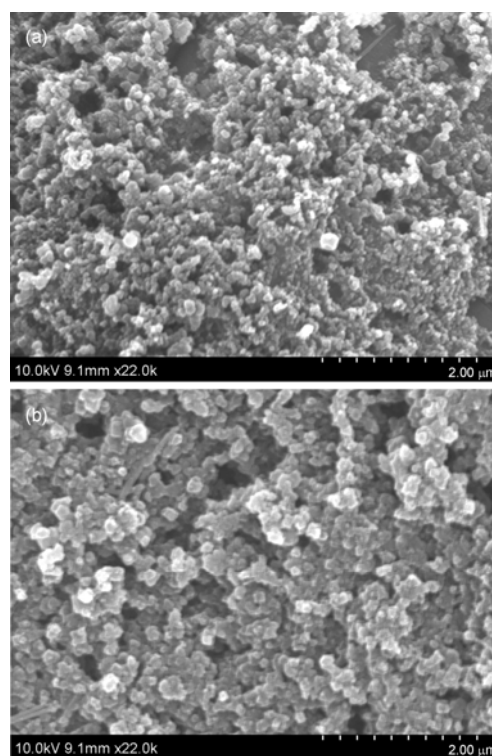| Component | Li metal | Separator | Cathode |
|---|---|---|---|
| Discharge capacity (mAh g⁻¹) | 819 | 541 | 27 |



**Figure 6** SEM images of the cathode with 5 wt% α-MnO₂ before discharge (a) and after discharge (b).

## 3  Conclusions

The α-MnO₂ hollow clews assembled with nanowires are successfully synthesized by a simple redox reaction of KMnO₄ and MnSO₄. This α-MnO₂ is an efficient catalyst for Li-air batteries which improves the cycleability greatly. Based on the results of Li-air batteries by re-assembling them with the used lithium metal foil, separators and cathode separately, we can reasonably conclude that the cathode is the most important factor to end the battery life. Reducing

the polarization of the cathode is crucial to improve the performance of rechargeable Li-air batteries.

1    Ogasawara T, Debart A, Holzapfel M, et al. Rechargeable $Li_2O_2$ electrode for lithium batteries. J Am Chem Soc, 2006, 128: 1390–1393

2    Sandhu S S, Fellner J P, Brutchen G W. Diffusion-limited model for a lithium/air battery with an organic electrolyte. J Power Sources, 2007, 164: 365–371

3    Abraham K. A brief history of non-aqueous metal-air batteries. J Electrochem Soc, 2008, 3: 42–67

4    Abraham K M, Jiang Z. A polymer electrolyte-based rechargeable lithium/oxygen battery. J Electrochem Soc, 1996, 143: 1–5

5    Lu Y C, Gasteiger H A, Parent M C, et al. The influence of catalysts on discharge and charge voltages of rechargeable Li-oxygen batteries. Electrochem Solid St, 2010, 13: A69–A72

6    Lu Y C, Kwabi D G, Yao K P C, et al. The discharge rate capability of rechargeable $Li-O_2$ batteries. Energy Environ Sci, 2011, 4: 2999–3007

7    Zhang X Y, Fang S H, Zhang Z X, et al. $Li/LiFePO_4$ battery performance with a guanidinium-based ionic liquid as the electrolyte. Chin Sci Bull, 2011, 56: 2906–2910

8    Oh S M, Oh S W, Yoon C S, et al. High-performance carbon-$LiMnPO_4$ nanocomposite cathode for lithium batteries. Adv Funct Mater, 2010, 20: 3260–3265

9    Armand M, Tarascon J M. Building better batteries. Nature, 2008, 451: 652–657

10   Bruce P G. Energy storage beyond the horizon: Rechargeable lithium batteries. Solid State Ionics, 2008, 179: 752–760

11   Ellis B, Lee K, Nazar L. Positive electrode materials for Li-ion and li-batteries. Chem Mater, 2010, 22: 691–714

12   Girishkumar G, McCloskey B, Luntz A C, et al. Lithium-air battery: Promise and challenges. J Phys Chem Lett, 2010, 1: 2193–2203

13   Kowalczk I, Read J, Salomon M. Li-air batteries: A classic example of limitations owing to solubilities. Pure Appl Chem, 2007, 79: 851–860

14   Padbury R, Zhang X. Lithium-oxygen batteries—limiting factors that affect performance. J Power Sources, 2011, 196: 4436–4444

15   Song M-K, Park S, Alamgir F M, et al. Nanostructured electrodes for lithium-ion and lithium-air batteries: The latest developments, challenges, and perspectives. Mater Sci Eng R, 2011, 72: 203–252

16   Kraytsberg A, Ein-Eli Y. Review on Li-air batteries-opportunities, limitations and perspective. J Power Sources, 2011, 196: 886–893

17   Débart A, Bao J, Armstrong G, et al. An $O_2$ cathode for rechargeable lithium batteries: The effect of a catalyst. J Power Sources, 2007, 174: 1177–1182

18   Zhang D, Fu Z, Wei Z, et al. Polarization of oxygen electrode in rechargeable lithium oxygen batteries. J Electrochem Soc, 2010, 157: A362–A365

19   Xu W, Viswanathan V V, Wang D Y, et al. Investigation on the charging process of $Li_2O_2$-based air electrodes in $Li-O_2$ batteries with organic carbonate electrolytes. J Power Sources, 2011, 196: 3894–3899

20   Débart A, Paterson A, Bao J, et al. $\alpha$-$MnO_2$ nanowires: A catalyst for the $O_2$ electrode in rechargeable lithium batteries. Angew Chem Int Edit, 2008, 47: 4521–4524

21   Zhang G, Zheng J, Liang R, et al. $\alpha$-$MnO_2$/carbon nanotube/carbon nanofiber composite catalytic air electrodes for rechargeable lithium-air batteries. J Electrochem Soc, 2011, 158: A822–A827

22   Read J. Characterization of the lithium/oxygen organic electrolyte battery. J Electrochem Soc, 2002, 149: A1190–A1195

23   Jin L, Xu L, Morein C, et al. Titanium containing $\gamma$-$MnO_2$ (Tm) hollow spheres: One-step synthesis and catalytic activities in Li/air batteries and oxidative chemical reactions. Adv Funct Mater, 2010, 20: 3373–3382

24   Crisostomo V M B, Ngala J K, Alia S, et al. New synthetic route, characterization, and electrocatalytic activity of nanosized manganite. Chem Mater, 2007, 19: 1832–1839

25   Cheng H, Scott K. Carbon-supported manganese oxide nanocatalysts for rechargeable lithium-air batteries. J Power Sources, 2010, 195: 1370–1374

26   Li J, Wang N, Zhao Y, et al. $MnO_2$ nanoflakes coated on multi-walled carbon nanotubes for rechargeable lithium-air batteries. Electrochem Commun, 2011, 13: 698–700

27   Wang X, Li Y. Selected-control hydrothermal synthesis of $\alpha$-and $\beta$-$MnO_2$ single crystal nanowires. J Am Chem Soc, 2002, 124: 2880–2881